Journal of Applied Electrochemistry (2005) 35:709–714
DOI 10.1007/s10800-005-5166-y

Modeling of the photocatalytic decomposition of gaseous benzene in a TiO_2 coated optical fiber photoreactor

W. WANG[1], Y. KU[1,*], C.M. MA[1] and F.T. JENG[2]
[1]*Department of Chemical Engineering, National Taiwan University of Science and Technology, 43, Keelung Road, Section 4, Taipei, 106, Taiwan*
[2]*The Graduate Institute of Environmental Engineering, National Taiwan University, 71, Chou-Shan Road, Taipei, 106, Taiwan*
*(*author for correspondence, e-mail: ku508@mail.ntust.edu.tw)*

Received 29 June 2004; accepted in revised form 06 February 2005

Key words: coating thickness, Langmuir–Hinshelwood surface kinetics, optical fiber photoreactor, quantum yield, reactor design equation, TiO_2

Abstract

Photocatalytic decomposition of benzene in an air stream in a continuous TiO_2-coated optical fiber photoreactor (OFP) was demonstrated to be effective at relatively short retention times. An increase in TiO_2 coating thickness, fiber length and retention time improved the decomposition of benzene; however, excessive TiO_2 coating thickness and optical fiber length may hamper the reaction. The UV light intensity distribution on and within the optical fiber was modeled using Snell's law and UV light energy balance. The modeled profile indicated that the UV light intensity decreased rapidly along the axial and radial directions of the optical fiber. A mathematical model combining the continuity equations and Langmuir–Hinshelwood surface kinetics was established to adequately describe the reaction behavior of benzene decomposition in the OFP with only single TiO_2-coated fiber.

Nomenclature

α	UV light attenuation coefficient of optical fiber at wavelength of 365 nm (cm^{-1})
ε	extinction coefficient of the TiO^2 film (nm^{-1})
ω	Fresnel reflection coefficient of optical fiber
δ	thickness of the TiO^2 film (nm)
θ	incident angle of UV light into material (optical fiber, cladding layer)
ϕ_b	apparent quantum yield of benzene decomposition
ϕ_c	apparent quantum yield of benzene mineralization to CO_2 generation
ϕ_c^*	normalized apparent quantum yield of CO_2 generation
η_m	eigen-value of partial differential equation
C_A	concentration of gaseous benzene in air stream (ppmv)
C_{Ao}	initial concentration of gaseous benzene in the photoreactor (ppmv)
D_{AB}	diffusion coefficient of benzene ($cm^2\ s^{-1}$)
I_o	Bessel function in the integrated form
$I_{f(z)}$	UV light intensity in the TiO_2 coating layer at position z ($W\ m^{-2}$)
I_{fo}	UV light intensity irritated into the optical fiber ($W\ m^{-2}$)
k_i	intrinsic photocatalytic reaction rate constant (mmole min^{-1})
K	adsorption equilibrium constant of benzene on TiO_2 particle ($ppmv^{-1}$)
L	length of optical fiber in photoreactor (cm)
m	natural number in summation formula
n	reaction order of applied UV light intensity
r	position of the optical fiber in radial direction (mm)
r_i	radius of the naked optical fiber (mm)
r_o	radius of the TiO_2 coated optical fiber (mm)
R_A	photocatalytic decomposition rate of gaseous benzene (ppmv min)
t	time (min)
v_z	velocity of air stream in z axial direction ($cm\ s^{-1}$)
z	position of the optical fiber in axial direction (cm)

1. Introduction

Photocatalytic oxidation has been demonstrated to be an effective technology for treating trace levels of organic pollutants in air stream [1–4]. However, the practical application of the UV/TiO_2 process is restricted by the development of photoreactors. Hoffmann et al. [5] and Peral et al. [6] have reviewed various types of photoreactor capable for the application of UV/TiO_2 process. Hung and Marinas [7] and Herrmann et al. [8] also reported that fixed-bed reactors with coated TiO_2 film on the irradiated surface are the most commonly used

photoreactors for its ease on operation either in the gaseous phase or aqueous solution. The optical fiber reactor (OFP) has been shown to be a potential alternative to conventional photoreactors due to its unique configuration.

The application of OFP for the decomposition of organic pollutants was initially proposed by Marinangeli and Ollis [9] to analyze the light intensity profile on optical fibers and evaluate the feasibility of OFPs in large scale operation. Peill and Hoffmann [10] further characterized OFP systems and established the Langmuir–Hinshelwood kinetic model coupled with light intensity distribution for interpreting the photocatalysis of 4-chlorophenol in aqueous solution. Choi et al. [11] proposed a simplified model correlated with light reflections in fiber core to describe the light intensity attenuation along the optical fiber. Furthermore, Peill and Hoffmann [10], Choi et al. [11] and Wang and Ku [12] have employed the Langmuir–Hinshelwood kinetics combined with one-dimensional light intensity attenuation for the modeling of reaction occurred in an OFP.

The modeling of UV intensity distribution within a photoreactor has been studied for various geometries of OFPs [10, 11, 13] for decomposition of organic contaminants. The interaction of coating thickness and fiber length for the light delivery in a TiO_2 coated fiber was modeled by Wang and Ku [14]. However, few researches have focused on light flux transfer within the coated photocatalyst layer and the flow pattern within photoreactors that are crucial in the design of OFPs.

2. Experimental

Chemicals and gases used in this study were reagent-grade purchased from major chemical companies and utilized without any further purification. The immobilization and characterization of TiO_2 coated on the 1.0 mm diameter fused silica optical fibers (Shanghai Optical Communication, Q4–1.0 N) were reported in our previous study [12, 14]. The total coated area for a 20 cm-long optical fiber was determined to be about 157 mm^2. The TiO_2-coated fibers were then exposed to ozone-containing humid air stream for 30 min to eliminate any organic compounds adhered on the surface of the coated fiber. A 20 cm-long Pyrex tubing of 0.4 cm inside diameter with a volume of 2.356 cm^3 with oily single TiO_2-coated fiber located at the centerline of the tubing was used as photoreactor for experiments in this study. The schematic diagram of the reactor is shown in Figure 1. The UV light emitted from a xenon arc UV lamp (Oriel 6263, 500 W maximum output primarily at 365 nm wavelength) was magnified and projected on the tip of the single coated fiber by a focusing-lens module. The temperature of photoreactor system was kept at 25 °C by for all experiments.

Benzene-laden air stream was prepared by extracting vapor from liquid benzene with dewatered compressed air. Air stream was kept at 40 °C by wrapping a flexible electric heating tape around the pipeline to avoid condensation of benzene and humidity, and led to flow through the OFP reactor for about 20 min to saturate the benzene adsorption by coated TiO_2 before experiment was conducted. The UV light source was warmed up for 5 to 10 min to achieve a steady light output before it irritated on the tip of the optical fiber. Outlet gas samples were taken after the temperature, gas flow rate, pressure, UV light intensity and humidity in the photoreactor system were steady; usually, the time required was less than 30 min. After each experimental run, humid ozone-containing air stream was introduced to the reactor for 30 min with UV light source on, in order to destroy any organic intermediates deposited on the inner surface of OFP. A China Chromatography 9800F gas chromatograph equipped with a flame ionization detector (FID) and an OIC model 700 non-dispersible infrared detector (NDIR) analyzer were used to determine the concentrations of benzene and CO_2 of the outlet air stream, respectively.

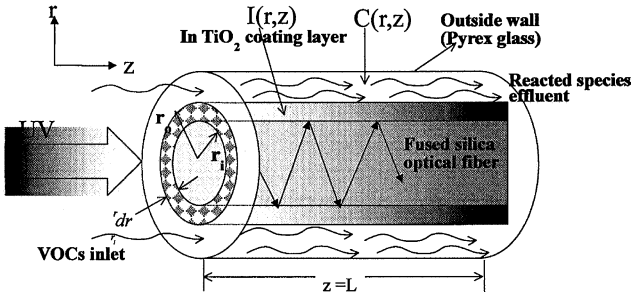

Fig. 1. Schematic diagram of the optical fiber photoreactor used in this study.

3. Result and discussion

3.1. *Modeling the light transmission within the TiO_2 layer coated on optical fiber*

The light transmission within an optical fiber was initially studied by Marinangeli and Ollis [9]. According to the Snell's law and Fresnel's law [14], the reflection or refraction of light is supposed to be bounded within the optical fiber and only a minimal portion of UV light can be emitted out of the TiO_2 coating. The conservation equation of radiant energy at a given wavelength around a TiO_2-coated optical fiber operated isothermally at steady-state could be established in z and r directions for cylindrical coordinates shown as follows:

$$\frac{1}{r}\frac{\partial}{\partial r}\left(r\frac{\partial I_f}{\partial r}\right)+\frac{\partial^2 I_f}{\partial z^2}=0$$
$$I_f=f(r,z)\, r_i \le r \le r_0, 0 \le z0 \le L \qquad (1)$$

where I_f is the light intensity in the TiO_2 coating layer at z direction. There are four boundary conditions of Equation (1) corresponded to light intensity (I_f). However, the

residual light intensity measured at the fiber-tip related to the fiber length (L) and thickness of TiO_2 coating layer ($\delta = r - r_i$) have been identified in our previous study [14] and boundary conditions were set as:

$$I_f = \omega \cdot \varepsilon \cdot I_{fo} e^{-[\alpha z]} \quad \text{at } r = r_i \tag{2}$$

$$I_f = 0 \quad \text{at } z = L \tag{3}$$

$$I_f = I_{fo} \quad \text{at } z = 0 \tag{4}$$

$$I_f = \omega \cdot \varepsilon \cdot I_{fo} e^{-[\alpha z + \varepsilon(r_o - r_i)]} = f(z) \quad \text{at } r = r_o \tag{5}$$

where ω is the Fresnel reflection coefficient related to fiber length, ε is the extinction coefficient of TiO_2 layer, α is the attenuation coefficient of the naked optical fiber, I_{fo} is the incident light intensity and $(r_0 - r_i)$ is the thickness of TiO_2 coating layer. The 2D non-homogeneous PDE was solved and shown as dimensionless light intensity in the TiO_2 coating layer related to coating thickness and fiber length can be calculated via the following equation resolved from Equation (1):

$$\frac{I_f(r,z)}{I_{fo}} = \left(\frac{2 \cdot \omega \cdot \varepsilon}{L} \cdot e^{-\varepsilon(r_o - r_i)}\right) \cdot \sum_{m=1}^{\infty} \frac{I_o(\eta_m r)}{I_o(\eta_m r_o)} \cos(\eta_m z) \cdot \left[\frac{1 - \omega \cdot e^{-\alpha \cdot L}\left(\alpha \cdot \cos\frac{(2m-1)\pi}{2} - \eta_m \sin\frac{(2m-1)\pi}{2}\right)}{\alpha^2 + {\eta_m}^2}\right] \tag{6}$$

where η_m is the eigen-value of the partial differential equation and equal to $\frac{(2m-1)\pi}{2L}$. The analytical solution of light intensity distribution obtained by Equation (6) indicates that light intensity distribution is function of both fiber length (Z) and TiO_2 thickness ($r_o - r_i$) with an exponential decay. Due to the complicated expression of light intensity distribution on optical fiber, Equation (6) can be simplified and rearranged as:

$$\frac{I_{fo}}{I_f(r,z)} = \frac{\xi}{1 + \beta \cdot e^{-\alpha}} \tag{7}$$

where

$$\beta = \omega^{-1} \cdot \left(\alpha \cdot \cos\frac{(2m-1)\pi}{2} - \eta_m \sin\frac{(2m-1)\pi}{2}\right)^{-1} \tag{8}$$

$$\xi = \left(\frac{2 \cdot \omega \cdot \varepsilon}{L} \cdot e^{-\varepsilon(r_o - r_i)}\right)^{-1} \cdot \sum_{m=1}^{\infty} \frac{I_o(\eta_m r_o)}{I_o(\eta_m r)} \sec(\eta_m z) \cdot (\alpha^2 + {\eta_m}^2) \tag{9}$$

3.2. *Modeling the benzene concentration profile in the OFP*

The performance of an optical fiber reaction system for the degradation of a single compound was modeled by combining the Langimuir–Hinshelwood kinetics with light transmission model mentioned above. For a differential-type optical fiber reactor operated isothermally at steady state, assuming the density and diffusivity of air stream is constant, the diffusion inside the TiO_2 layer is negligible, the conservation equation could be established by a simplified Navier–Stoke continuity equation shown as follow:

$$v_z \frac{\partial C_A}{\partial z} = D_{AB}\left(\frac{1}{r}\frac{\partial}{\partial r}\left(r\frac{\partial C_A}{\partial r}\right) + \frac{\partial^2 C_A}{\partial z^2}\right) \tag{10}$$

where C_A is the concentration of benzene, v_z is the flow rate of the benzene-laden air stream in z direction, D_{AB} is the diffusivity of benzene. The air stream flow in the reactor is assumed to be plug flow with no concentration gradient in θ direction. The boundary conditions are shown as follow:

$$C_A = C_{A0} \quad \text{at } z = 0 \tag{11}$$

$$D_{AB}\left(\frac{\partial C_A}{\partial r}\right) = -R_A \quad \text{at } r = r_i \tag{12}$$

$$\frac{\partial C_A}{\partial r} = 0 \quad \text{at } r = 0.4\,\text{cm} \tag{13}$$

Equation (11) indicates that the benzene concentration at the entrance of reactor is kept uniform and steady. Equation (12) addresses that the mass-transferred benzene is completely decomposed in the OFP. The rate expression for a heterogeneous photocatalytic reaction is described by Langmuir–Hinshelwood kinetic expression:

$$-R_A = -k \cdot \frac{K \cdot C_A}{1 + K \cdot C_A} \tag{14}$$

where K is the dynamic adsorption constant and k is the apparent reaction rate constant and a function of UV light intensity.

$$k = k_i \cdot I_f^n \tag{15}$$

where k_i is the intrinsic reaction rate constant, n is the reaction order with respect to the applied UV light intensity, I_f. The continuity equation for benzene in cylindrical coordinate in an ideal plug flow reactor operated in steady state is expressed as Equation (13):

$$-\frac{\partial C_A}{\partial \tau} = -R_A = \left(\frac{k K C_A}{1 + K C_A}\right) \tag{16}$$

By integrating the above equation and regressing with the data for experiments conducted with various initial benzene concentrations, the K value can be determined. Equation (10) was then solved numerically to predict the concentration distribution of benzene decomposition in the differential OFP.

3.3. *Experimental findings and model fittings*

Thickness of TiO_2 coatings covered on the fiber surface is an important parameter for the operation of photocatalytic reactor owing to its specific roles on UV light transmission and photocatalytic reaction. Figure 2 depicts the SEM micrographs of TiO_2 coatings of different thickness covered on the optical fiber used in this study. Irregular stacking of TiO_2 particles on the fiber surface was found for coatings developed from higher TiO_2 slurry contents, which might inhibit the UV light transmission along the fiber according to our previous study [14].

The effect of TiO_2 coating thickness on the photocatalytic decomposition of benzene in the OFP can be modeled adequately by Equation (1) for experiments conducted with various UV light intensities, as shown in Figure 3. The decomposition of benzene was increased for experiments conducted with thicker TiO_2 coating, especially under the application of higher UV irradiating intensities. However, Chen et al. [15] reported that the excessive thickness of TiO_2 layer (>1.0 μm) might increase the resistances of both UV light delivery and reactant transfer.

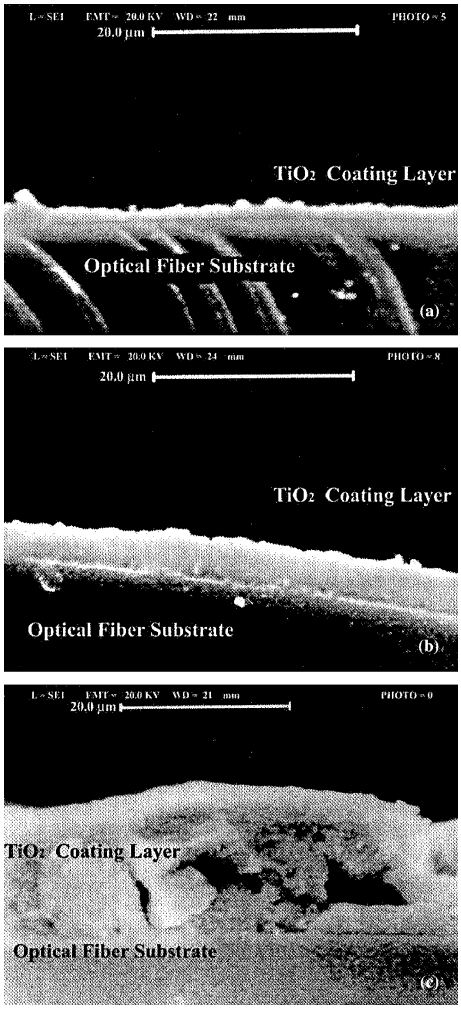

Fig. 2. Cross-sectional SEM micrograph of the TiO_2 coating on 1-mm diameter fused silica optical fiber from solution containing (1) 2.5 wt% of TiO_2(2) 10.0 wt% of TiO_2 (3) 20.0 wt% of TiO_2.

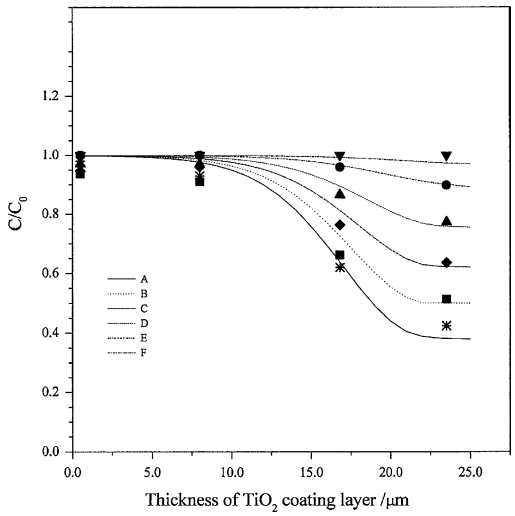

Fig. 3. Effect of TiO_2 coating thickness on the benzene decomposition by photocatalytic oxidation in the OFP operated at various light intensities: 10 ppmv benzene, 100 ml min^{-1} flow rate, 30% humidity: key (*), (■), (◆), (▲), (●) and (▼) were experimental result at I 2716, 2139, 1562, 985, 408, 120 W m^{-2}: (A), (B), (C), (D), (E) and (F) were simulation values at I = 2716, 2139, 1562, 985, 408, 120 W m^{-2}.

Table 1 depicts the apparent quantum yields of benzene decomposition (ϕ_b) and CO_2 production (ϕ_{c*}) for experiments conducted in an OFP covered with TiO_2 coating of various thickness. The apparent quantum yield calculated in this study is defined as the difference of organic concentration (ΔC_A) in a constant volume (V) divided by the incident light intensity of 365 nm (I_{abs}) entered a fiber times the irradiation time interval (Δt) rather than the emitting intensity of light source used commonly by other researchers [16, 17]. The definition of apparent quantum yields (ϕ_b and ϕ_c) are expressed, respectively, as below:

$$\phi_b = \frac{\text{moles of benzene disappeared}}{\text{moles ofphotons absorbed}} \cong \frac{\Delta C_A \cdot V}{I_{abs}/U_{\lambda=365\,nm} \cdot \Delta t} \tag{17}$$

$$\phi_c = \frac{\text{moles of } CO_2 \text{ produced}}{\text{moles ofphotons absorbed}} \cong \frac{\Delta C_A \cdot V}{I_{abs}/U_{\lambda=365\,nm} \cdot \Delta t} \tag{18}$$

Table 1. Apparent quantum yields of benzene decomposition and mineralization by photocatalytic oxidation in the OFP coated with various TiO_2 thicknesses

Effect of TiO_2 thickness		
TiO_2 thickness/μm	ϕ_b^1	ϕ_c^{*2}
0.5	5.41×10^{-3}	0
8.0	9.28×10^{-3}	1.55×10^{-4}
16.8	2.94×10^{-2}	1.11×10^{-2}
23.5	4.224×10^{-2}	0.0188

Relative humidity = 30%. Flow rate = 100 ml min^{-1}.

where the ($U_{\lambda=365\ nm}$) (3.28×10^5 Joule Einstein^{-1}) is the energy per mole of photons at wavelength of 365 nm, and I_{abs} is calculated via Equation (7). For comparing the (ϕ_b) and (ϕ_c) through mass balance of carbon, (ϕ_c) were divided by 6 because benzene composed of six carbon atoms. Hence the normalized (ϕ_c, ϕ_{c*}) is defined as:

$$\phi_c^* = \phi_c/6 \tag{19}$$

Both the apparent quantum yields of benzene decomposition and CO_2 production were increased with the TiO_2 coating thickness, possibly because more surface sites available for the adsorption of organic species. The amount of CO_2 production was increased significantly with TiO_2 coating thickness possibly due to the favorable adsorption of hydrophilic organic intermediates on illuminated TiO_2 surface [12, 18]. However, some researchers [11] noticed that the reaction rate of photocatalysis might be reduced for experiments conducted with excessive amounts of TiO_2 coating because the penetration of emitted light and mass transfer of organic species were inhibited.

As shown in Figure 4, the photocatalytic decomposition of benzene in the OFP increased linearly with retention time of the gas stream for experiments conducted with various incident light intensities. Similar results reported by Wang et al. [19] for photocatalytic decomposition of trichloroethylene in a packed-bed photoreactor. The calculated quantum yields of benzene decomposition (ϕ_b) and CO_2 production (ϕ_{c*}) were found to be decreased with increasing airflow rates as shown in Table 2, indicating that more organic intermediates were generated for experiments conducted with higher airflow rates. Therefore, the quantum yield of CO_2 production decreased more significantly with increasing airflow rates than the quantum yield of benzene decomposition.

Table 2. Apparent quantum yields of benzene decomposition and mineralization by photocatalytic oxidation in the OFP operated at various retention times

Effect of flow rate		
Retention time/s[3]	ϕ_b	ϕ_c^*
14.364	4.79×10^{-2}	2.29×10^{-2}
2.8727	2.74×10^{-2}	9.90×10^{-3}
1.4137	1.56×10^{-2}	3.18×10^{-3}
0.9425	1.13×10^{-2}	2.27×10^{-3}
0.7069	8.66×10^{-3}	9.73×10^{-4}

Relative humidity = 30%. Thickness of TiO_2 coating = 16.8 μm.

As shown in Figure 5, the photocatalytic oxidation of benzene for experiments conducted in photoreactors with optical fiber of different length and gaseous flow rates in the range of 50–300 ml min^{-1}. The decomposition of benzene decreased obviously with the length of optical fiber for experiments conducted with various gaseous flow rates. The apparent quantum yield was calculated and was also found to be increased with the length of optical fiber for experiments conducted in photoreactors with optical fiber coated with various TiO_2 thicknesses as revealed in Figure 6. However, both Figures 5 and 6 indicate that the effect of fiber length merely enhanced the decomposition of benzene and apparent quantum yield for optical fiber length greater than 10 cm. It is possibly due to the decay of light intensity along the TiO_2 coated optical fiber. Previous studies have addressed that light intensity decays exponentially along the fiber, the photocatalytic reaction was assumed to occur mainly at the front region of an OFP [18].

As depicted in Figure 7, both the quantum yields of benzene decomposition (ϕ_b) and mineralization (ϕ_c*) were increased for experiments conducted in photoreactors with longer fibers, especially under UV

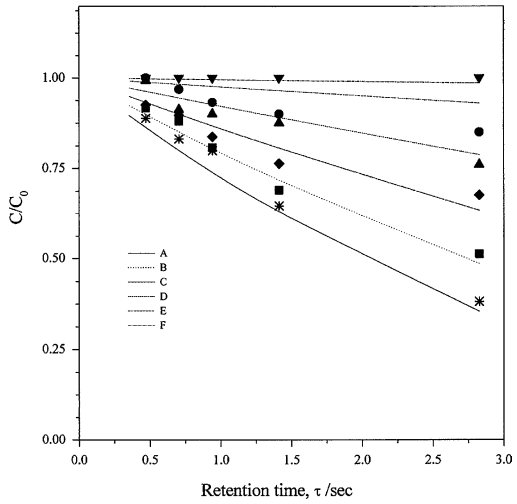

Fig. 4. Effect of retention times (τ) on the benzene decomposition by photocatalytic oxidation in the OFP operated at various light intensities: 10 ppmv benzene, 100 ml min^{-1} flow rate, 30% humidity: key (*), (■), (◆), (▲), (●) and (▼) were experimental result at I 2716, 2139, 1562, 985, 408, 120 W m^{-1}:(A), (B), (C), (D), (E) and (F) were simulation values at I = 2716, 2139, 1562, 985, 408, 120 W m^{-2}.

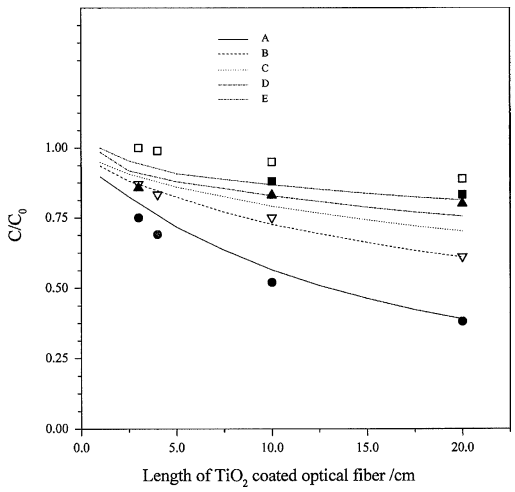

Fig. 5. Effect of fiber length on the benzene decomposition by photocatalytic oxidation in the OFP operated at various gaseous flow rates: 10 ppmv benzene, 2716 light intensity W m^{-2}, 16.8 μm TiO_2 coating thickness: key (●), (▽), (▲), (■) and (□) were experimental values at flow rate = 50, 100, 150, 200, 250 ml min^{-1}: (A), (B), (C), (D) and (E) were simulation result at flow rate = 50,100,150, 200, 250 ml min^{-1}.

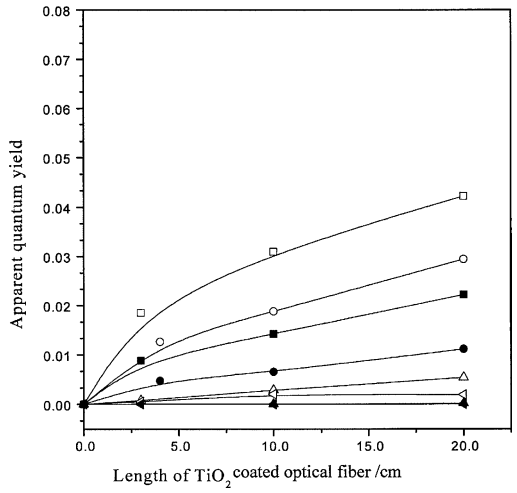

Fig. 6. Effect of fiber length on the apparent quantum yields of decomposition (ϕ_b) and mineralization (ϕ_c^*) of benzene by photocatalytic oxidation in the OFP coated with various TiO_2 coating thickness: 10 ppmv benzene, 2716 light intensity W m^{-2}, 100 flow rate ml min^{-1}: key (□), (○), (△), (◁) were ϕ_b at TiO_2 coating thickness = 23.5, 16.8, 8.0, 0.5 μm, (■), (●), (▲), (◀) were ϕ_c^* TiO_2 at coating thickness = 23.5, 16.8, 8.0, 0.5 μm.

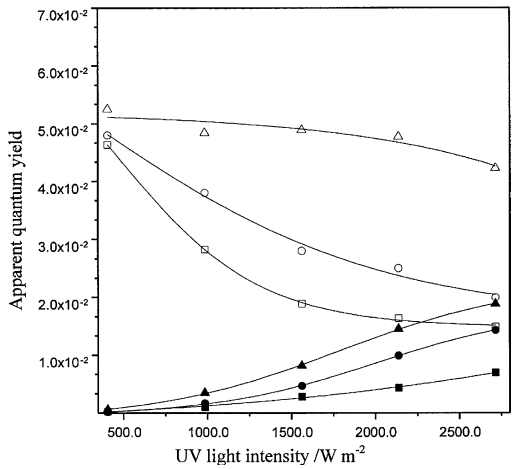

Fig. 7. Effect of light intensity on the apparent quantum yields of decomposition (ϕ_b) and mineralization (ϕ_c^*) of benzene by photocatalytic oxidation in the OFP operated at various lengths of optical fiber: 10 ppmv benzene, 23.5 μm TiO_2 coating thickness, 100 flow rate ml min^{-1}: key (□), (○), (△) were ϕ_b at lengths of optica1 fiber = 3.0, 10.0, 20.0 cm, (■), (●), (▲) were ϕ_c^* at lengths of optical fiber = 3.0, 10.0, 20.0 cm.

light irradiation of higher intensities. The (ϕ_b) was decreased with light intensity while the (ϕ_c*) was increased inversely. It is probably because the UV illuminated TiO_2 surface is hydrophilic and favorable for the adsorption of reaction intermediates [16, 22]. Non-polar hydrophobic benzene molecules and hydrophilic intermediates, such as phenol and formic acid, might compete the active sites on the surface of TiO_2. The light intensity disfribution model depicted as Equation (7) can be coupled with Equations (17) and (18) to model the effect of light intensity on (ϕ_b) and (ϕ_c*) as shown in Figure 7.

4. Conclusion

The photocatalytic oxidation of gaseous benzene in a single fiber, continuous flow TiO_2-coated optical fiber reactor was revealed to be effective for experiments conducted at relatively short retention times. The increase of TiO_2 coating thickness, fiber length and retention time of gas flow in OFP can improve the decomposition of benzene; however, for experiments conducted with TiO_2 coating thickness of greater than 23.5 μm or fiber length longer than 10.0 cm, the photocatalytic decomposition of benzene were hampered. The modeled profile based on Snell's law and UV light energy balance indicated that UV light intensity decreased rapidly along the axial and radial directions of the optical fiber, UV light diffracted within the optical fiber was primarily consumed at the fiber/TiO_2 interface. The photocatalytic decomposition of gaseous benzene along the optical fiber reactor could be properly described by the proposed design equation combining the light distribution consideration and Langmuir–Hinshelwood surface kinetics.

Acknowledgement

This research was supported by Grant NSC-91–2211-E011–022 from the National Science Council, Taiwan, Republic of China.

References

1. D.F. Ollis and H. Al-Ekabi, *Photocatalytic Purification and Treatment of Water* (Elseiver, Amsterdam, The Netherlands, 1993), pp. 481.
2. A.L. Linsebigler, L. Guangquan and J.T. Tates, *Chem. Rev.* **3** (1995) 735.
3. X. Fu, W.A. Zeltner and M.A. Anderson, *Appl. Catal. B: Environ.* **6** (1995) 209.
4. N.N. Lichtin and M. Sadeghi, *Photochem. Photobiol. A: Chem.* **113** (1998) 81.
5. M.R. Hoffmann, S.T. Martin, W. Choi and D.W. Bahnemann, *Chem. Rev.* **95** (1995) 69.
6. J. Peral, X. Domenech and J.D.F. Ollis, *Chem. Technol. Biotechnol.* **70** (1997) 117.
7. C.H. Hung and B.J. Marinas, *Environ. Sci. Technol.* **31** (1997) 561.
8. J.M. Herrmann, H. Tahiri, Y. AitIchou, G. Lassaletta, E. Gonzalez and A.R.A. Fernandez, *Appl. Catal. B Environ.* **13** (1997) 219.
9. R.E. Marinangeli and D.F. Ollis, *AIChE. J.* **28** (1982) 945.
10. N.J. Peill and M.R. Hoffmann, *Environ. Sci. Technol.* **32** (1998) 398.
11. W. Choi, J.Y. Ko, H. Park and J.S. Chung, *Appl. Catal. B: Environ.* **31** (2001) 209.
12. W. Wang and Y. Ku, *J. Photobiol. Photochem.* **159** (2003) 47.
13. R-D. Sun, A. Nakajima, I. Watanabe, T. Watanabe and K. Hashimoto, *J. Photochem. Photobiol. A: Chem.* **136** (2000) 111.
14. W. Wang and Y. Ku, *Chemosphere* **50** (2003) 999.
15. D. Chen, F. Li and A.K. Ray, *AIChE J.* **46** (2000) 1034.
16. I. Ilisz, Z. Zsuzsanna Laszlo and A. Dombi, *Appl. Catal. A.* **18** (1999) 25.
17. R.G. Changrani and G.B. Raupp, *AIChE J.* **46** (2000) 829.
18. A. Fujishima, T.N. Rao and D.A. Tryk, *J. Photochem. Photobiol. C: Photochem. Rev.* **1** (2000) 1.
19. K.H. Wang, H.H. Tasi and Y.H. Hsieh, *Appl. Cata. B: Environ.* **17** (1998) 313.